

AVR2004: LC-Balun for AT86RF230

Features

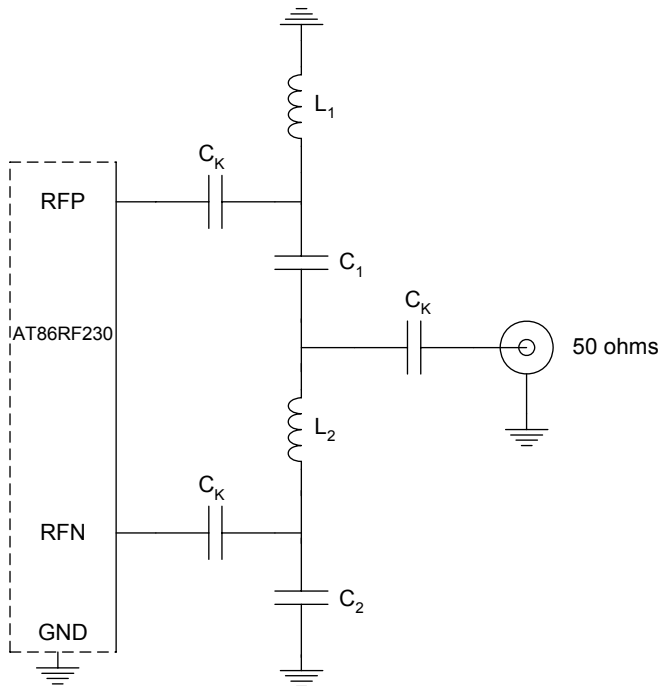
- Balun for AT86RF230 with lumped elements
- Simulation results
- S-Parameter file

1 Introduction

In some cases the used balun on the ATAVR[®]RZ502 Radio Boards must be replaced by concentrated elements. Therefore the functionality must be given by the use of capacitors and inductors only. This application note shows how to transform the differential AT86RF230 RF signal into a single-ended 50 ohm antenna without using the original balun.

To convert a differential signal to a single-ended type, a *balanced* to *unbalanced* transformation has to be done by using a *balun* circuit. For this transformation, hand calculation, simulation, hardware, real measurements and the resulting S-Parameter file are shown and given.

Figure 1-1. Schematic of a balun structure attached to AT86RF230



Application Note

Rev. 8113A-AVR-04/08



2 General Considerations

The task to solve is to transform a RF signal from a differential port, which are two signals relating to each other, into a signal which is related to ground level (a single-ended port). Since the common balun structure is a reciprocal element, it is possible to change input port with output port and still get the same functionality. So if a signal from a single-ended port is the input signal, the balun structure has to transform it to a signal on a differential port. Therefore the input signal must be turned into two non-ground signals. This can be done by using a low pass branch and a high pass branch generating a $+90^\circ$ and a -90° signal. Using this as a differential signal fulfills the desired needs. As an initial step the capacitor and inductor values for the branches can be calculated following Equation 2-1, as a starting point for balun simulations at 2.45GHz. Consider the capacitors C_K from Figure 1-1 as DC blocking elements, therefore a value of 22pF is enough.

Equation 2-1. Simple balun equation set

$$R_{inner} = \sqrt{R_{IN} R_{OUT}} = \sqrt{100\Omega \cdot 50\Omega} \approx 71\Omega$$

$$L_1 = L_2 = \frac{R_{inner}}{2 \cdot \pi \cdot f} = 4.6nH$$

$$C_1 = C_2 = \frac{1}{2 \cdot \pi \cdot f \cdot R_{inner}} = 0.92pF$$

3 Simulation

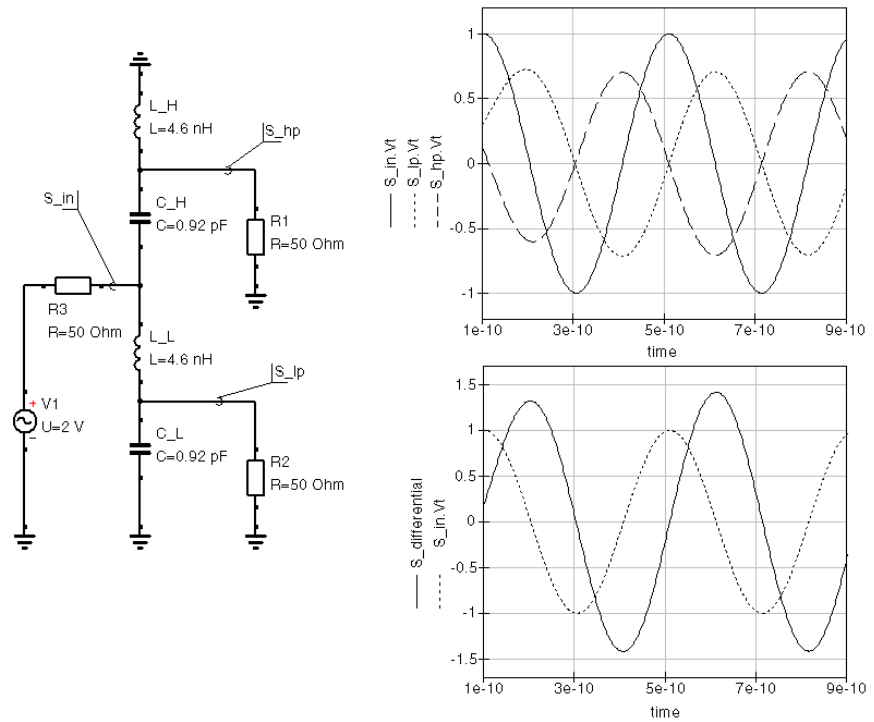
For simulation purposes, several software tools do exist. To enable the reader to use the S-Parameter file from the measurements, the freeware *Quite Universal Circuit Simulator* [1] was used here.

The circuit for the simulation consists of a low-pass branch (C_H and L_H) and a high-pass branch (L_L and C_L) as shown in Figure 3-1 using the calculated values from Equation 2-1. The single-ended source $V1$ feeds both branches at their series input elements. The output signals S_{hp} for the high-pass branch and S_{lp} for the low-pass branch are plotted in Figure 3-1 and shall be seen as two signals shifted by ± 90 degrees compared to the input signal S_{in} .

Since the signals S_{hp} and S_{lp} do have a time constant phase difference following Equation 3-1, these two signals can be combined to the one desired differential signal.

The balun designer may take a look at the input and output impedance of the circuit, since it is the goal to interface other RF circuits and provide the best match to them. For this application note the differential port is the gate to the AT86RF230 pins RF_P and RF_N , the single ended port is connected to the single-ended antenna. So the differential impedance must have 100 ohms as the AT86RF230 datasheet states and the single ended port must have 50 ohms impedance, since a standard antenna should be used.

Figure 3-1. Simulation of the balun principle

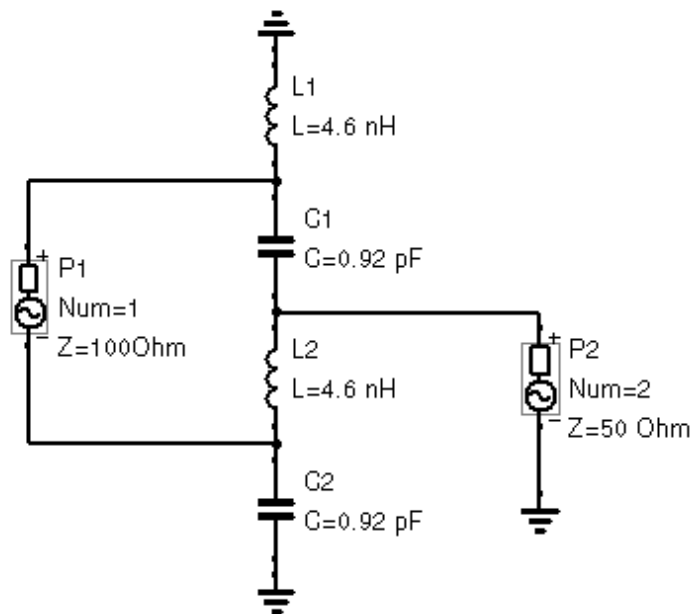


Equation 3-1. resulting differential phase

$$Phase_1 - Phase_2 = Phase_{differential}$$

$$+ 90^\circ - (-90^\circ) = +180^\circ$$

Figure 3-2. Simulated circuit



When the circuit as shown in Figure 3-2 is simulated at 2450MHz, which is almost the middle frequency of the 2.4GHz ISM-band, the input impedance measured at the differential port P1 is 100 ohms and the output impedance at port P2 is 50 ohms as desired and shown in Figure 3-3 and Figure 3-4, inclusive the 180° phase shift expressed as 0° phase shift due to the differential impedance view at port P1.

Figure 3-3. Simulation result, magnitude and phase of input and output impedance in [ohm] and [°]

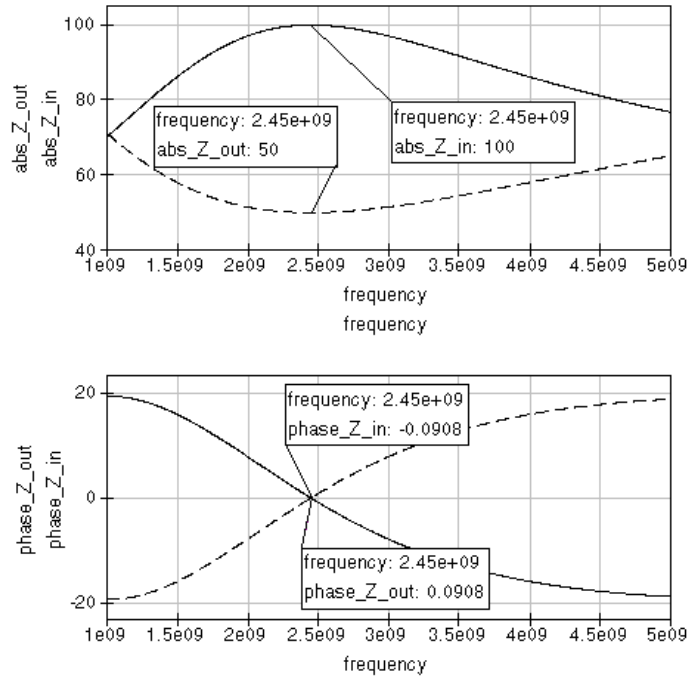
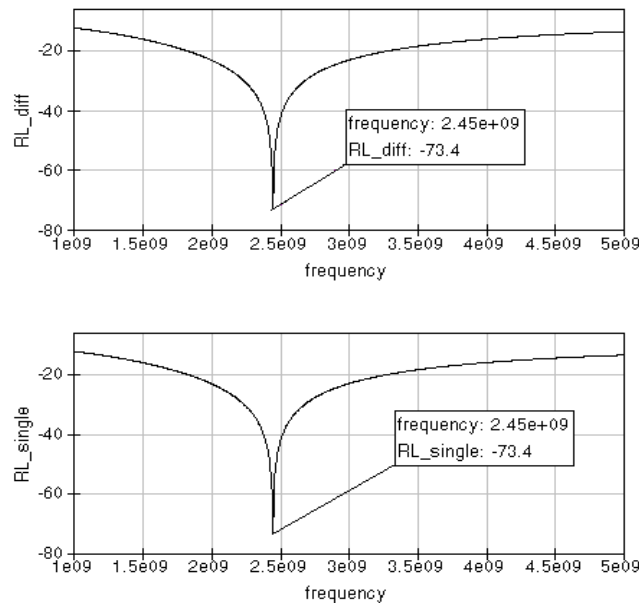


Figure 3-4. Simulation result, return loss of balun ports in [dB]

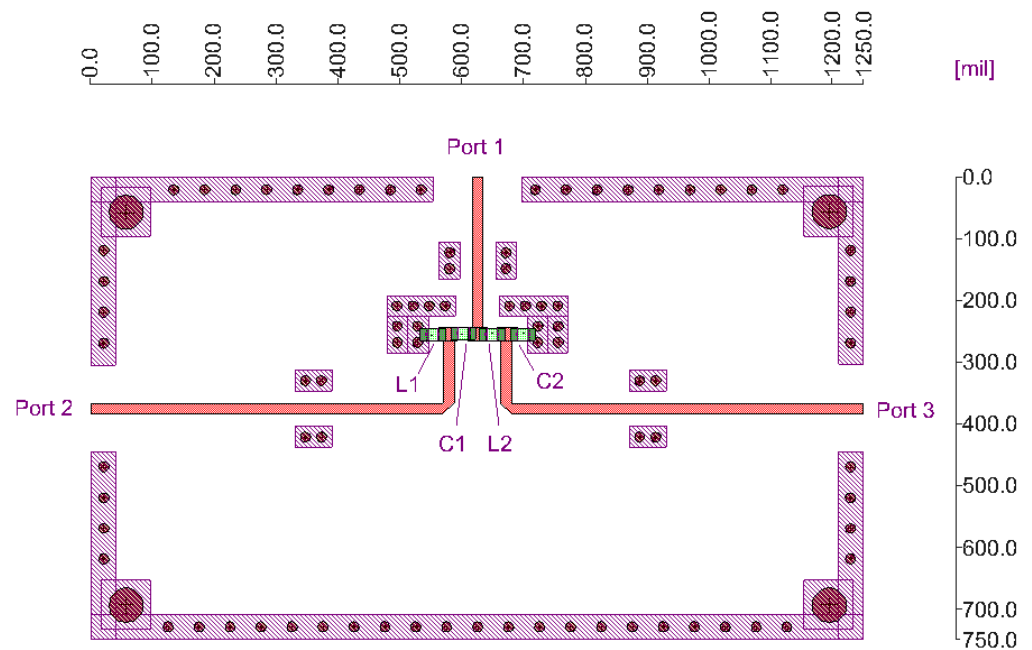


4 Test Device

4.1 Layout

For the circuit from Figure 3-2, a PCB was designed. The layout is shown in Figure 4-1. The PCB's material is Rogers 4003 instead of FR4 to extract the S-parameter of this circuit as exactly as possible. The reason for this is, that Rogers 4003 provides a more static ϵ_r than FR4 does. At the end the S-parameters of this circuit were recalculated to deembed the traces of the PCB, from the PCB borders up to the pads of the SMD components.

Figure 4-1. Test PCB



4.2 Measurements

To ensure the measured values rely on the circuitry only, the board was measured without the SMD components first. Therefore the traces were measured single-ended from the PCB border when the end of each trace was grounded, to find the electrical length.

After knowing the influence of each trace to the circuit, the measurements of the complete structure with populated components were done. Since this may be done later again with other measurement devices, the procedures were limited to basic 50-ohm two-port equipment only. So, no three- or four-port measurement devices were used. To measure a balun with a two-port network analyzer, the third and unused port has to be loaded with a 50 ohm match. This ends up in two *.s2p files, but one *.s3p file is needed. Therefore the popular software MathCAD® was used for crunching the two *.s2p files to one standard *.s3p file.

Based on that result and the measurements, the traces were deembedded. The results of this procedure are shown in Figure 4-2, Figure 4-3 and Figure 4-4 as the desired parameters.

Figure 4-2 shows the input return loss at common port in dB. The other ports 2 and 3 are terminated with a 50 ohm match to the ground node, which is equivalent to 100 ohms differential impedance between both of these ports.

Figure 4-2. Input return loss of s11 (common port)

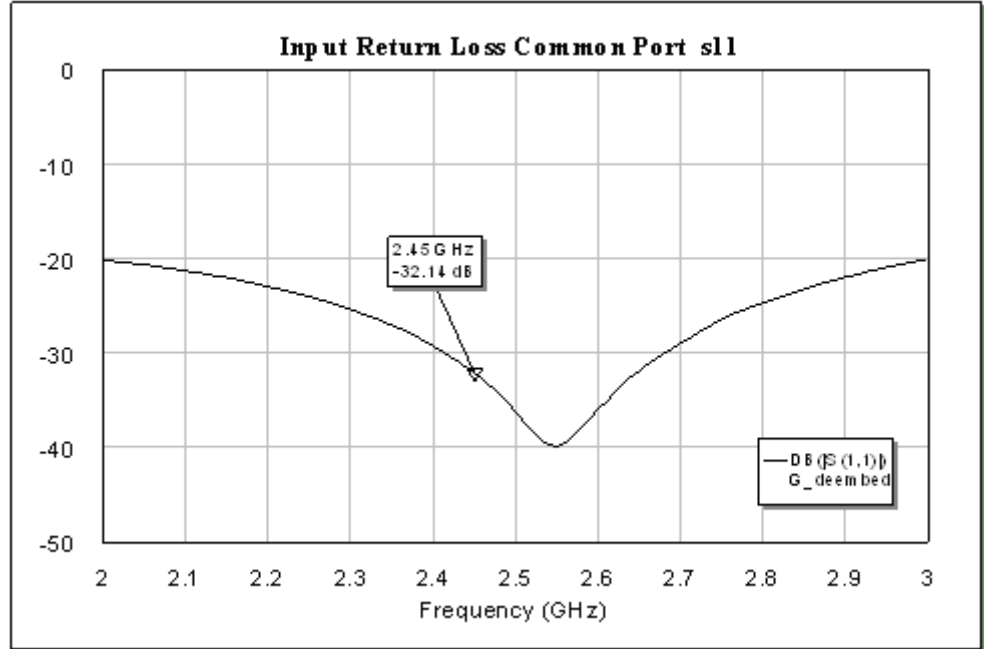


Figure 4-3. Magnitude curves of s21 and s31 (differential ports)

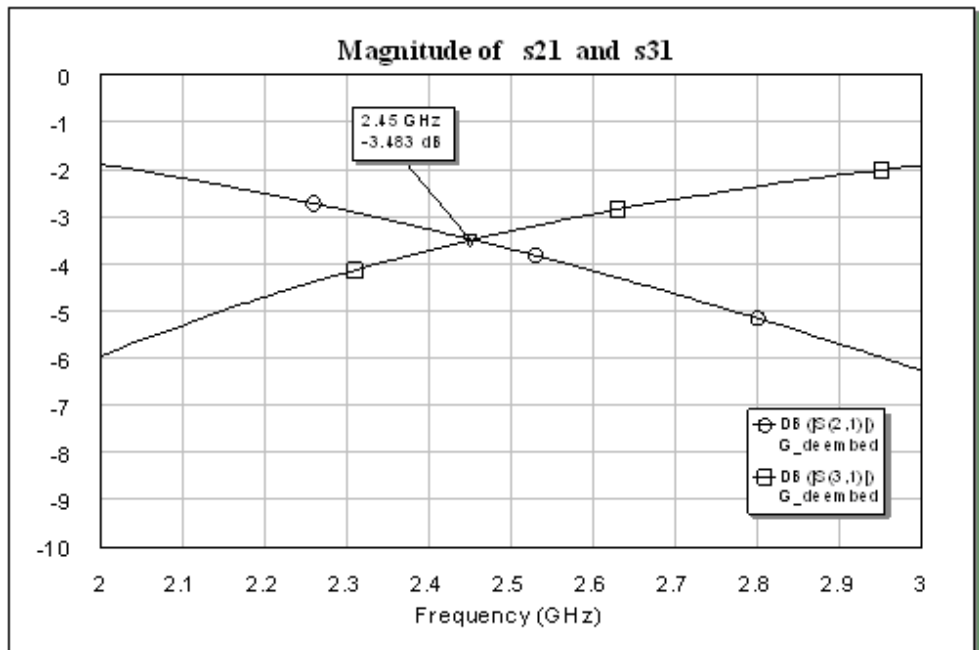
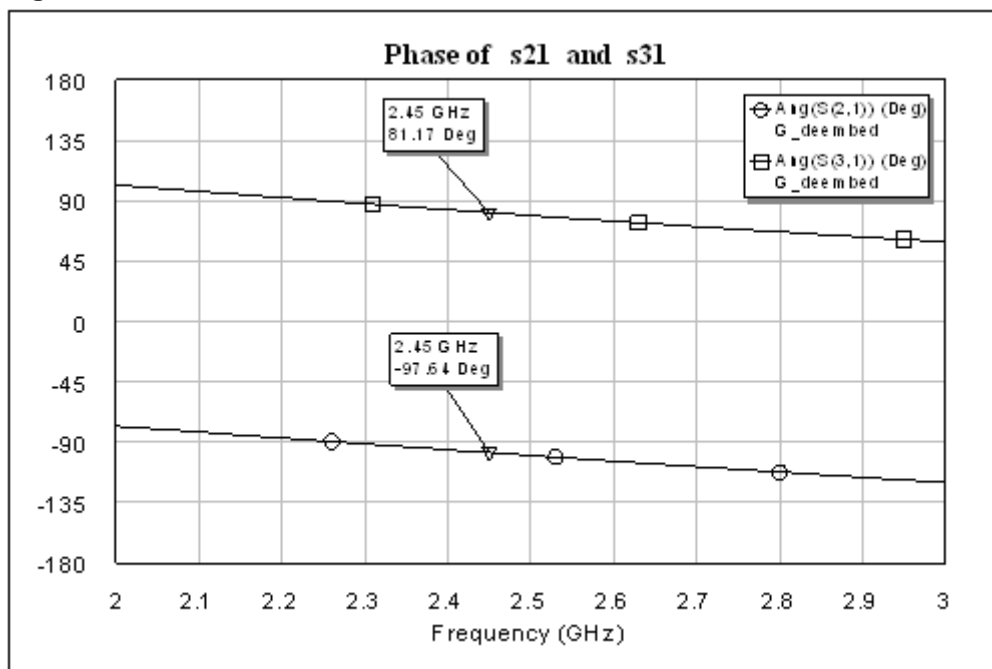


Figure 4-4. Phase curves of S21 and S31



The transmission parameter's magnitudes in dB are shown in Figure 4-3, with S21 marked with circles and S31 with squares. The low-pass and high-pass functions of the appropriate LC networks and the crossover frequency at band center frequency (2.45 GHz) can be observed.

Figure 4-4 shows the transmission parameter phase in degrees. The S21's phase is marked with circles and S31's phase with squares. The differential phase of approximately 180 degrees can be observed at band center frequency (2.45 GHz).

The first measurement showed a shifted cross-over frequency, so slightly changes to the component values were necessary. This fine-tuning during consecutive measurements did lead to slightly different values than hand calculation and early simulations showed. The results are given in Table 4.1. Since these results show reflection coefficients of -30dB, the developed circuit fulfils the AT86RF230 needs.

Table 4-1. measurement results compared to simulated values

component	Simulated value	Measured value
C1 = C2	0.92 pF	0.82 pF
L1 = L2	4.6 nH	4.3 nH
Best impedance match	2.45 GHz	2.57 GHz
Reflection coefficient at 2.45 GHz (differential port)	-73.4 dB	-31.2 dB
Reflection coefficient at 2.45 GHz (single-ended port)	-73.4 dB	-31.5 dB



4.3 S-Parameter

The S-parameter of the LC balun for the AT86RF230 comes with this application note as zip file, downloadable at Atmel's website www.atmel.com.

With a circuit, as shown in Figure 4-5, the parameters can be experienced as shown in Figure 4-6.

Figure 4-5. Simulation circuit to extract parameters

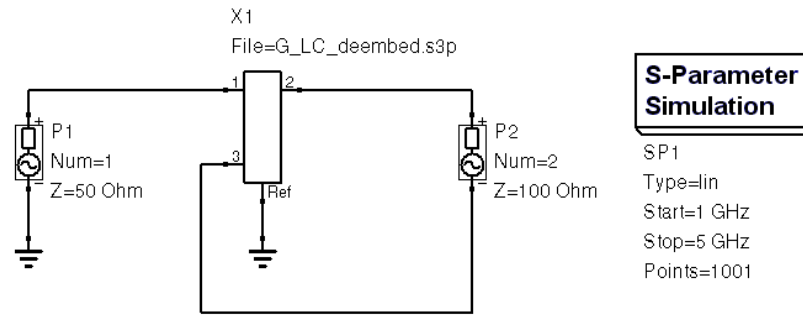
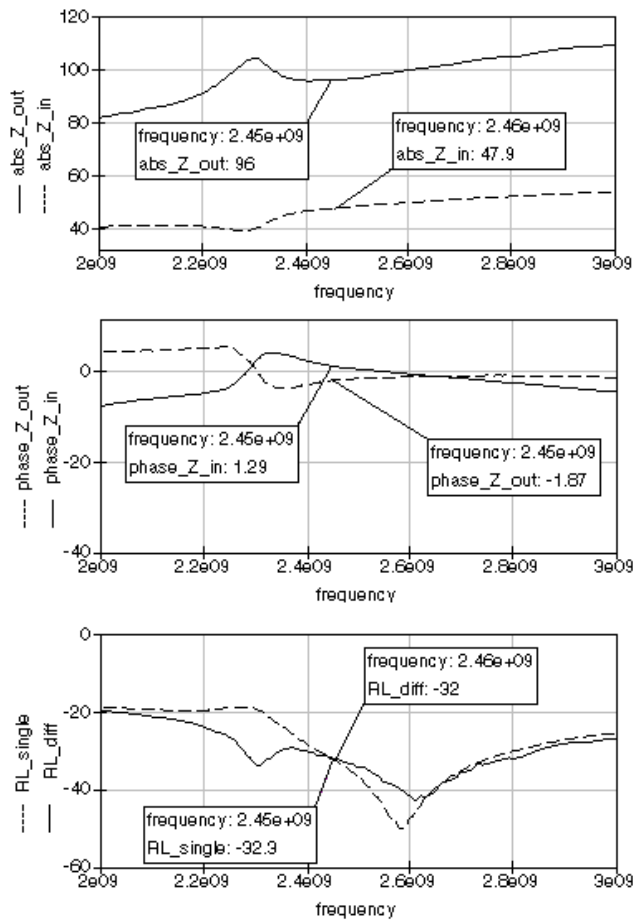


Figure 4-6. Parameters extracted from measured s3p file in [ohm], [°] and [dB]



5 Harmonics

Due to its non-linearity behavior, a RF device transmits not only at the main or center frequency. RF energy is also detectable at integer multiples of the center frequency, which are called *harmonics*. A device transmitting at a center frequency $f_c = 2.45\text{GHz}$ will also radiate RF energy at $2 \times f_c = 4.9\text{GHz}$, $3 \times f_c = 7.35\text{GHz}$, and so on. A good RF transmitter radiates as much of its transmitting power at center frequency as possible and therefore as less energy as possible at the harmonic frequencies. International and national regulatory instances like FCC or ETSI limit the power radiations at all frequency bands. The power level limit from FCC for the harmonic frequencies 4.9GHz, 7.35GHz and 9.8GHz is -41.2dBm and ETSI limits the radiation on harmonics to -30dBm.

The used hardware to measure the harmonic power levels was an ATAVRRZ502 Radio Board on STK[®]501/STK500 combination. The interesting fact here is, that an AT86RF230 IC was chosen, which provides as much RF output power as possible to be as close at the regulatory limits as possible or above. The chosen AT86RF230 provided 4dBm output power, which is more than the specified +/-3dBm. For this “too good” IC it was expected that the harmonics are increased in the same way. Table 5-1 shows the measured power levels of the used hardware.

Table 5-1. Measurement results, harmonic power level on “too good” AT86RF230 with balun from Wuerth Electronics

frequency	Channel 11	Channel 15	Channel 26
2.45GHz	4.06 dBm	3,99 dBm	3,96 dBm
4.9GHz	-40.78 dBm	-41,94 dBm	-44,68 dBm
7.35GHz	-40.24 dBm	-41,12 dBm	-42,49 dBm
9.8GHz	-47.84 dBm	-47,42 dBm	-47,77 dBm

A second ATAVRRZ502 Radio Board was chosen, providing about the same RF output power as the Wuerth balun Radio Board, for populating the above developed LC-Balun instead of the standard balun from Wuerth Electronics. For this case, inductors from Murata were used ($L=4.3\text{nH}$, 0402, Murata LQG15HN4N3S02) and capacitors from Phycomp ($C=0.82\text{pF}$, NP0, 0402, Phycomp, SPLR 223886915827, RS Comp. 616-9357). The circuit from Figure 5-1 was used to measure the harmonic power. The results are shown in Table 5-2.

Figure 5-1. LC-Balun circuit for power measurement at harmonics

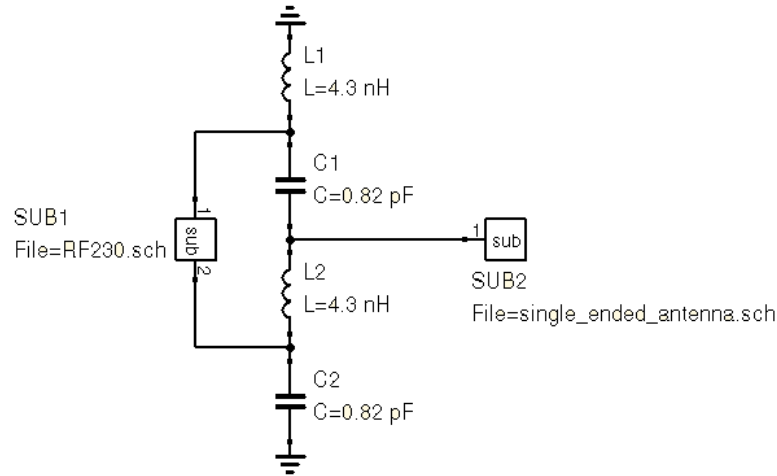


Table 5-2. Measurement results of harmonic power level on “too good” AT86RF230 with LC-balun

frequency	Channel 11	Channel 15	Channel 26
2.45GHz	4,22 dBm	4,14 dBm	3,98 dBm
4.9GHz	-36,07 dBm	-35,62 dBm	-34,78 dBm
7.35GHz	-33,54 dBm	-33,81 dBm	-32,73 dBm
9.8GHz	-53,67 dBm	-53,2 dBm	-53,7 dBm

Table 5-3. Harmonics power of LC-balun above FCC

frequency	Channel 11	Channel 15	Channel 26
2.45GHz	n/a	n/a	n/a
4.9GHz	5,13 dB	5,58 dB	6,42 dB
7.35GHz	7,66 dB	7,39 dB	8,47 dB
9.8GHz	0 dB	0 dB	0 dB

From Table 5-1 and Table 5-2 it can be seen, that both baluns radiate more power than the FCC limits allow, but less enough to fulfill the ETSI limits. It is not surprising that the Wuerth balun shows this behavior. The Radio Board was designed to operate slightly below the FCC limits, to provide the maximum output power at the antenna. This was done taking into account that the harmonics are slightly below FCC limits also. Now the “too good” AT86RF230 was used, with more output power than the sold AT86RF230 ICs, to show exactly this behavior.

The LC-Balun consists of a low-pass and a high-pass branch. Here the high-pass branch operates as it is defined. It passes higher frequencies than the center frequency it was designed for. This behavior is of course bad for the harmonics. So as expected, the attenuation of the AT86RF230 harmonics is less than the attenuation of the Wuerth-Balun.

Table 5-4. Harmonics power of Wuerth balun above FCC

frequency	Channel 11	Channel 15	Channel 26
2.45GHz	n/a	n/a	n/a
4.9GHz	0,42 dB	0 dB	0 dB
7.35GHz	0,96 dB	0,08 dB	0 dB
9.8GHz	0 dB	0 dB	0 dB

Table 5-3 and Table 5-4 provide the power levels above the FCC limits. This shows clearly, that a filter is needed. This filter has to provide at least an attenuation of 5.13dB at 4.9GHz and 7.66dB at 7.35GHz. For the Wuerth balun, this filter will work too, even if only 1dB would be necessary. Usable filters to solve this problem are the following types: Cauer, Bessel, Butterworth and Chebychev. A Chebychev filter was chosen and after dimensioning to a cutoff frequency of 3GHz, it provides attenuation of -17dB at $2 \times f_c$ as shown in Figure 5-3.

Figure 5-3. 3GHz Chebychev filter transmission function (absolute values) in [dB]

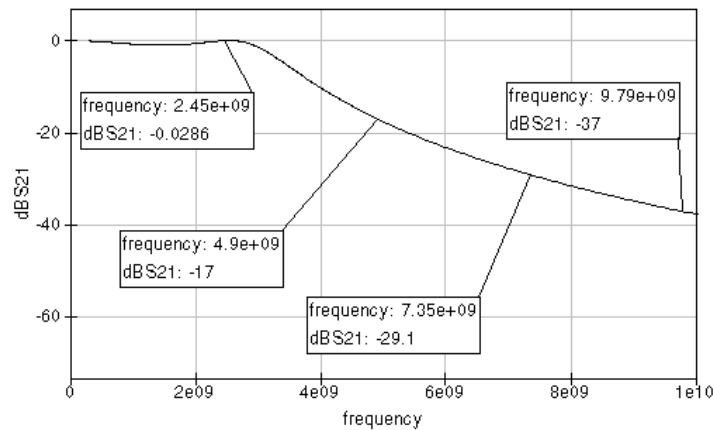


Figure 5-4. LC-Balun with 3GHz-Chebychev filter

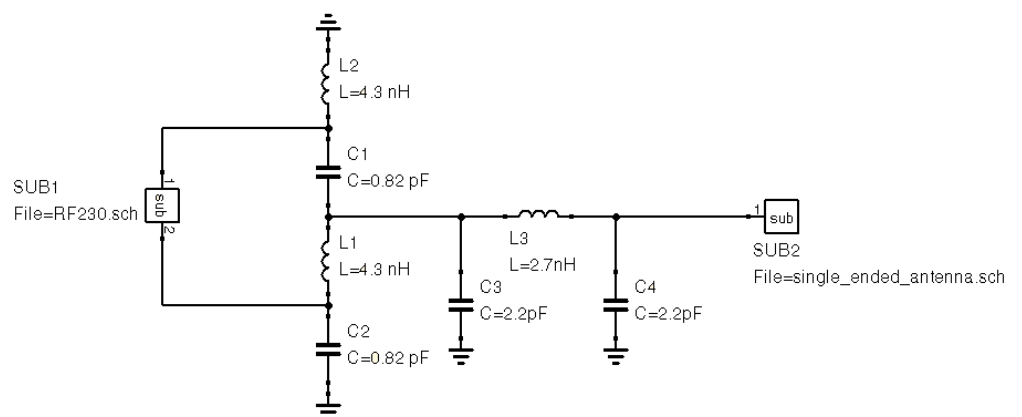


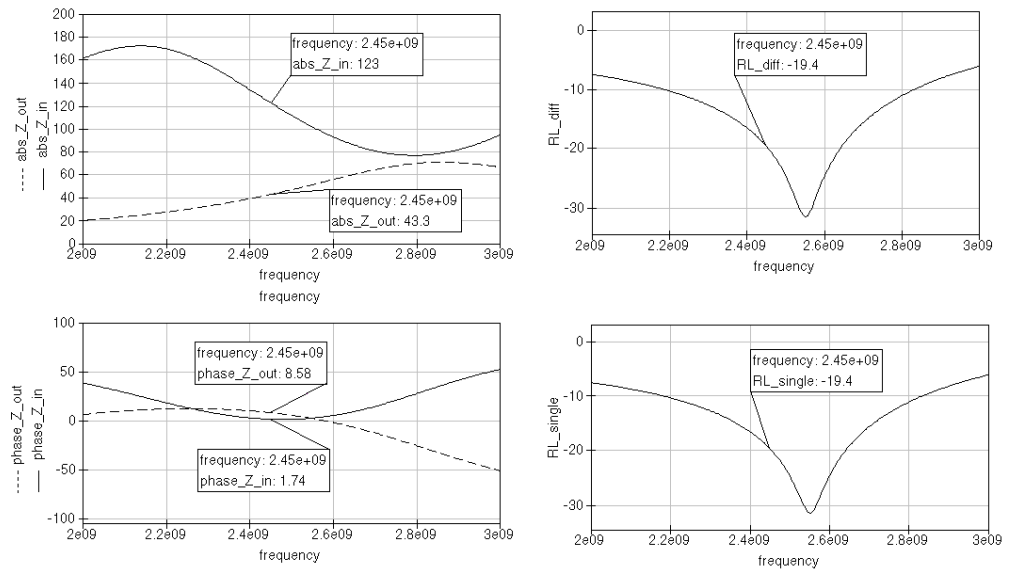
Table 5-5. Harmonics power level of LC-balun with applied filter

frequency	Channel 11	Channel 15	Channel 15
2.45GHz	4,1914 dBm	4,1114 dBm	3,9514 dBm
4.9GHz	-53,07 dBm	-52,62 dBm	-51,78 dBm
7.35GHz	-62,64 dBm	-62,91 dBm	-61,83 dBm
9.8GHz	-90,67 dBm	-90,2 dBm	-90,7 dBm

As it can be seen in Table 5.5, FCC limits are not hurt any longer with applied filter. ETSI limits were not hurt at all. For ETSI no filter would be needed, but the developed FCC filter will not disturb the functionality here, so finally one piece of hardware can be used to pass FCC and ETSI. The final schematic is provided in Figure 5-4.

The input and output impedances have changed a bit, but the matching at 2.45GHz is still good enough (better than 10 dB as AT86RF230 datasheet states). Figure 5-5 shows the simulated input impedance of the LC-Balun with applied filter, and the output impedance of the Chebychev filter, seen from a 50 ohms antenna.

Figure 5-5. overall impedance simulation results for LC-Balun with applied filter in [ohm] and [dB]



6 Common Mode Rejection Ratio

The Common Mode Rejection Ratio (CMRR) is a figure of merit, which describes the performance of a balanced circuit. It is defined as the ratio between the insertion loss of the differential mode versus the common mode with respect to signal gain following equation 6.1.

Equation 6-1. CMRR for balun circuit with port 1 as common port

$$CMRR = \frac{S_{1C}}{S_{1D}} = \frac{S_{12} + S_{13}}{S_{12} - S_{13}}$$

The developed LC balun showed a CMRR following Figure 6.1 and provides a CMRR based on measurement values of -36dB versus the Wuerth balun, as shown in Figure 6.2, which provides a CMRR of -29dB. So finally the developed LC circuit shows a better CMRR at the operating frequency band, but it does not help at all to prevent common mode signals at harmonic frequencies. The Wuerth balun shows a 12dB higher CMRR 4.9GHz, so finally the LC balun helps in operating space, but not more.

Figure 6-1. LC balun's CMRR in [dB]

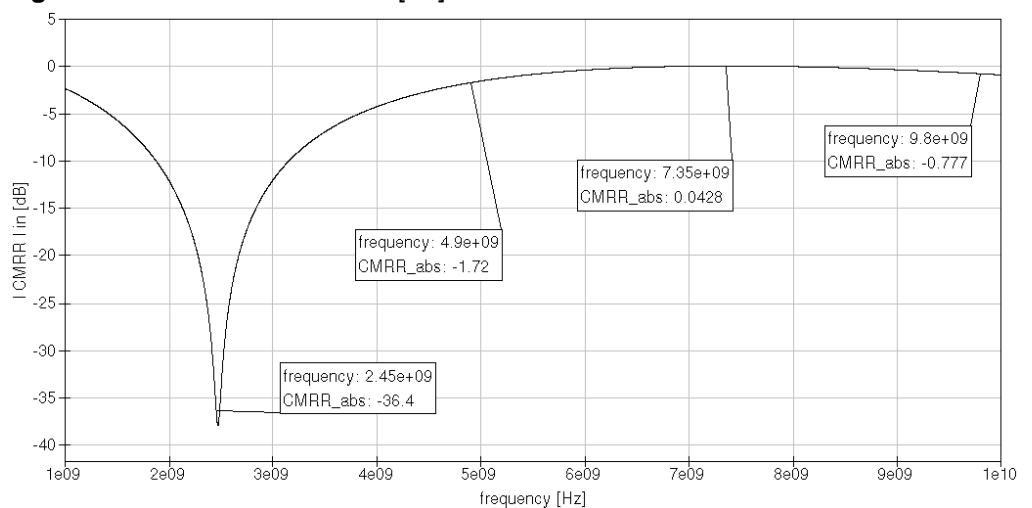
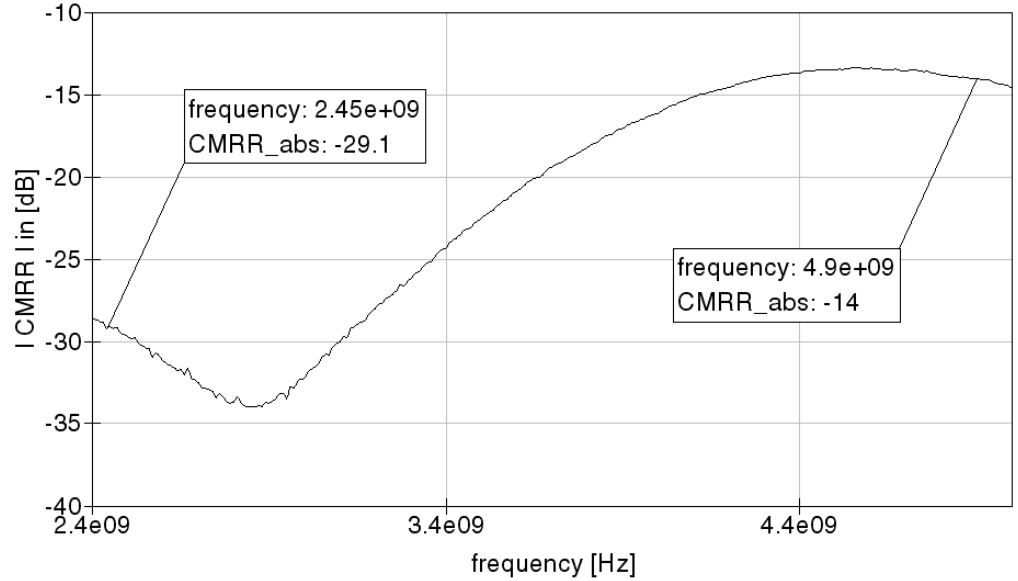


Figure 6-2. Wuerth balun's CMRR in [dB]



7 Conclusion

If the Wuerth balun, which is used on the ATAVRRZ502 Accessory Kit, must be replaced by a balun circuit consisting of lumped elements, one solution was shown here and measured in Atmel. The schematic can be found in Figure 5-4. As components for L1 and L2 Murata LQG15HN4N3S02 should be used and for the capacitors C1 and C2 Phycomp 223886915827 (RS Component Number: 616-9357) should be used. The LC balun has the disadvantage, that an additional filter must be used and the Common Mode Rejection is more worse than using the from Atmel recommended Wuerth balun as it is shown in the ATAVRRZ502 Accessory Kit.



Headquarters

Atmel Corporation
2325 Orchard Parkway
San Jose, CA 95131
USA
Tel: 1(408) 441-0311
Fax: 1(408) 487-2600

International

Atmel Asia
Room 1219
Chinachem Golden Plaza
77 Mody Road Tsimshatsui
East Kowloon
Hong Kong
Tel: (852) 2721-9778
Fax: (852) 2722-1369

Atmel Europe
Le Krebs
8, Rue Jean-Pierre Timbaud
BP 309
78054 Saint-Quentin-en-
Yvelines Cedex
France
Tel: (33) 1-30-60-70-00
Fax: (33) 1-30-60-71-11

Atmel Japan
9F, Tonetsu Shinkawa Bldg.
1-24-8 Shinkawa
Chuo-ku, Tokyo 104-0033
Japan
Tel: (81) 3-3523-3551
Fax: (81) 3-3523-7581

Product Contact

Web Site
www.atmel.com

Technical Support
avr@atmel.com

Sales Contact
www.atmel.com/contacts

Literature Request
www.atmel.com/literature

Disclaimer: The information in this document is provided in connection with Atmel products. No license, express or implied, by estoppel or otherwise, to any intellectual property right is granted by this document or in connection with the sale of Atmel products. **EXCEPT AS SET FORTH IN ATMEL'S TERMS AND CONDITIONS OF SALE LOCATED ON ATMEL'S WEB SITE, ATMEL ASSUMES NO LIABILITY WHATSOEVER AND DISCLAIMS ANY EXPRESS, IMPLIED OR STATUTORY WARRANTY RELATING TO ITS PRODUCTS INCLUDING, BUT NOT LIMITED TO, THE IMPLIED WARRANTY OF MERCHANTABILITY, FITNESS FOR A PARTICULAR PURPOSE, OR NON-INFRINGEMENT. IN NO EVENT SHALL ATMEL BE LIABLE FOR ANY DIRECT, INDIRECT, CONSEQUENTIAL, PUNITIVE, SPECIAL OR INCIDENTAL DAMAGES (INCLUDING, WITHOUT LIMITATION, DAMAGES FOR LOSS OF PROFITS, BUSINESS INTERRUPTION, OR LOSS OF INFORMATION) ARISING OUT OF THE USE OR INABILITY TO USE THIS DOCUMENT, EVEN IF ATMEL HAS BEEN ADVISED OF THE POSSIBILITY OF SUCH DAMAGES.** Atmel makes no representations or warranties with respect to the accuracy or completeness of the contents of this document and reserves the right to make changes to specifications and product descriptions at any time without notice. Atmel does not make any commitment to update the information contained herein. Unless specifically provided otherwise, Atmel products are not suitable for, and shall not be used in, automotive applications. Atmel's products are not intended, authorized, or warranted for use as components in applications intended to support or sustain life.

© 2008 Atmel Corporation. All rights reserved. Atmel®, logo and combinations thereof, AVR®, Z-Link® logo, STK® and others are the registered trademarks, and others are trademarks of Atmel Corporation or its subsidiaries. Other terms and product names may be trademarks of others.